THE JOURNAL OF BIOLOGICAL CHEMISTRY VOL. 290, NO. 8, pp. 4537–4544, February 20, 2015

F-ATPase of *Drosophila melanogaster* Forms 53-Picosiemen (53-pS) Channels Responsible for Mitochondrial Ca^{2+}-induced Ca^{2+} Release*

Received for publication, December 2, 2014, and in revised form, December 22, 2014
Published, JBC Papers in Press, December 30, 2014, DOI 10.1074/jbc.C114.629766

Sophia von Stockum[‡], Valentina Giorgio[‡], Elena Trevisan[‡], Giovanna Lippe[§], Gary D. Glick[¶], Michael A. Forte[‖], Caterina Da-Rè[**], Vanessa Checchetto[**], Gabriella Mazzotta[**], Rodolfo Costa[**], Ildikò Szabò[**], and Paolo Bernardi[‡1]

From the Departments of [‡]Biomedical Sciences and [**]Biology, University of Padova and Consiglio Nazionale delle Ricerche Neuroscience Institute, I-35131 Padova, Italy, the [§]Department of Food Science, University of Udine, I-33100 Udine, Italy, the [¶]Department of Chemistry, Graduate Program in Immunology, University of Michigan, Ann Arbor, Michigan 48109, and the [‖]Vollum Institute, Oregon Health and Sciences University, Portland, Oregon 97239

Background: The Ca^{2+}-induced Ca^{2+} release channel (mCrC) of *Drosophila* mitochondria is similar to the permeability transition pore (PTP).
Results: mCrC is modulated by PTP effectors and *Drosophila* F-ATPase forms 53-pS channels.
Conclusion: F-ATPase mediates Ca^{2+}-induced Ca^{2+} release in *Drosophila* mitochondria.
Significance: Channel formation by F-ATPases has been conserved in evolution, but species-specific features exist that may underscore different roles in different organisms.

Mitochondria of *Drosophila melanogaster* undergo Ca^{2+}-induced Ca^{2+} release through a putative channel (mCrC) that has several regulatory features of the permeability transition pore (PTP). The PTP is an inner membrane channel that forms from F-ATPase, possessing a conductance of 500 picosiemens (pS) in mammals and of 300 pS in yeast. In contrast to the PTP, the mCrC of *Drosophila* is not permeable to sucrose and appears to be selective for Ca^{2+} and H^+. We show (i) that like the PTP, the mCrC is affected by the sense of rotation of F-ATPase, by Bz-423, and by Mg^{2+}/ADP; (ii) that expression of human cyclophilin D in mitochondria of *Drosophila* S_2R^+ cells sensitizes the mCrC to Ca^{2+} but does not increase its apparent size; and (iii) that purified dimers of *D. melanogaster* F-ATPase reconstituted into lipid bilayers form 53-pS channels activated by Ca^{2+} and thiol oxidants and inhibited by Mg^{2+}/γ-imino ATP. These findings indicate that the mCrC is the PTP of *D. melanogaster* and that the signature conductance of F-ATPase channels depends on unique structural features that may underscore specific roles in different species.

Mitochondria of *Drosophila melanogaster* possess an array of Ca^{2+} transport pathways, *i.e.* the Ca^{2+} uniporter MCU, the Na^+/Ca^{2+} exchanger NCLX, and a Na^+-insensitive Ca^{2+} efflux system (1), that display the same features as those observed in mammalian mitochondria (2–5). An important difference, however, exists.

In mammalian mitochondria, Ca^{2+} and P_i induce opening of the permeability transition pore (PTP),[2] a 500-pS channel that forms from the F-ATPase under conditions of oxidative stress (6). The PTP is permeable to sucrose, as is the pore of yeast mitochondria (7, 8) where P_i has an inhibitory effect and F-ATPase forms 300-pS channels (9). Also in *D. melanogaster*, Ca^{2+} opens a mitochondrial permeability pathway, resulting in depolarization and Ca^{2+} release (1); however, this Ca^{2+}-induced Ca^{2+} release channel (mCrC, which like in yeast is inhibited rather than activated by P_i) is impermeable to sucrose, suggesting that its size may be considerably smaller than that of the PTP (1).

The recent demonstration that the PTP forms from the F-ATPase (6, 9) provides a new framework to analyze the nature of the mCrC of *D. melanogaster*. Here we have assessed whether F-ATPase dimers purified from *Drosophila* mitochondria possess channel activity. Our findings provide novel information on the channel function of F-ATPases, establish that the mCrC is the PTP of *D. melanogaster*, and shed new light on its possible role in regulation of Ca^{2+} homeostasis (10, 11).

EXPERIMENTAL PROCEDURES

Cell Cultures—Drosophila S_2R^+ cells (12, 13) were cultured in Schneider's insect medium (Life Technologies) supplemented with 10% heat-inactivated FBS (Life Technologies) and kept at 25 °C. Culture medium for the transfected S_2R^+pActCyPD-HA/pCoPuro cells was supplemented with 8 μg/ml puromycin.

Subcellular Fractionation—Cells were lysed in a medium containing 10 mM Tris-HCl, pH 6.7, 10 mM KCl, 150 μM $MgCl_2$ supplemented with protease and phosphatase inhibitor cocktails (Sigma) for 30 min on ice, followed by passage through a 26-gauge × 0.5-inch syringe (Artsana). Sucrose was then added at a final concentration of 250 mM, and lysates were centrifuged three times at 2,200 × *g* for 10 min at 4 °C to remove nuclei and cell debris. Mitochondria were then sedimented at 8,200 × *g* for 10 min at 4 °C.

Cell Permeabilization—Cells were detached with a sterile cell scraper, centrifuged at 200 × *g* for 10 min, and washed twice

* This work was supported in part by AIRC Grants IG13392 (to P. B.) and IG11814 (to I. S.), PRIN Programs 20107Z8XBW (to P. B.) and 2010CSJX4F (to I. S.), National Institutes of Health-Public Health Service Grant 1R01GM069883 (to M. F. and P. B.), and the University of Padova Progetti Strategici di Ateneo *Models of Mitochondrial Diseases* (to P. B.).
[1] To whom correspondence should be addressed: Dept. of Biomedical Sciences, University of Padova, Via Ugo Bassi 58/B, I-35121 Padova, Italy. Fax: 39-049-827-6049; E-mail: bernardi@bio.unipd.it.

[2] The abbreviations used are: PTP, permeability transition pore; pS, picosiemen(s); mCrC, mitochondrial Ca^{2+} release channel; BN-PAGE, blue native polyacrylamide gel electrophoresis; CyP, cyclophilin; CyPD, cyclophilin D; TOM20, translocase of outer mitochondrial membranes of 20 kDa; CsA, cyclosporin A; MCU, mitochondrial Ca^{2+} uniporter; CRC, Ca^{2+} retention capacity; OSCP, oligomycin sensitivity conferral protein; ctrl, control.

with 130 mM KCl, 10 mM Mops-Tris, pH 7.4 (KCl medium) containing 10 μM EGTA-Tris. The resulting pellet was resuspended in KCl medium containing 150 μM digitonin and 1 mM EGTA-Tris and incubated for 20 min on ice (6×10^7 cells $\times$ ml^{-1}). Cells were then diluted 1:5 in KCl medium containing 10 μM EGTA-Tris and centrifuged at 200 $\times$ *g* in a refrigerated centrifuge (4 °C) for 6 min. The final pellet was resuspended in KCl medium containing 10 μM EGTA-Tris at 4×10^8 cells $\times$ ml^{-1} and kept on ice.

Isolation of Mitochondria from Flies—Mitochondria were prepared from whole flies or 3rd instar larvae by differential centrifugation exactly as described (14).

Mitochondrial Membrane Potential and Ca^{2+} Retention Capacity—Mitochondrial membrane potential was measured using a Perkin-Elmer LS50B spectrofluorometer based on the fluorescence quenching of rhodamine 123 (15) at excitation and emission wavelengths of 503 and 523 nm, respectively, with the slit width set at 2.5 nm. Twenty million permeabilized S_2R^+ cells were added to the cuvette in a total volume of 2 ml. Further additions were as indicated in the figure legends. Extramitochondrial Ca^{2+} was measured based on Calcium Green 5N (Molecular Probes) fluorescence (15) at excitation and emission wavelengths of 485 and 538 nm, respectively, using a Fluoroskan Ascent FL plate reader (Thermo Scientific) with either 200 μg of isolated mitochondria or 2×10^6 permeabilized cells in a total volume of 200 μl/well. For measurements of Ca^{2+} retention capacity (CRC) and membrane potential during ATP synthesis at constant [ADP], the incubation medium contained 0.1 M glucose, 80 mM KCl, 10 mM Mops-Tris, pH 7.4, 5 mM succinate-Tris, 4 mM $MgCl_2$, 1 mM P_i-Tris, 0.5 mM $NADP^+$, 0.4 mM ADP-Tris, 50 μM P_1,P_5-di(adenosine-5′) pentaphosphate, 10 μM EGTA-Tris, 2 μM rotenone, 4 units/ml glucose-6-phosphate dehydrogenase, 3 units/ml hexokinase, and 0.5 μM Calcium Green 5N or 0.15 μM rhodamine 123. For measurements of CRC and membrane potential during ATP hydrolysis at constant [ATP], the incubation medium contained 0.1 M sucrose, 80 mM KCl, 10 mM Mops-Tris, pH 7.4, 4 mM $MgCl_2$, 2 mM phosphocreatine, 1 mM P_i-Tris, 0.4 mM ATP-Tris, 10 μM EGTA-Tris, 2 μM rotenone, 1.5 units/ml creatine kinase, and 0.5 μM Calcium Green 5N or 0.15 μM rhodamine 123. For all other measurements, the composition of the assay medium is specified in the figure legends, and further additions were as indicated.

Mitochondrial Swelling Assay—Absorbance at 540 nm was monitored with a Multiskan Ex (Thermo Scientific) plate reader. Either 200 μg of isolated mitochondria or 2×10^6 permeabilized cells were added to each well in a total volume of 200 μl. Incubation media are specified in the figure legends.

Fly Stocks and Breeding Conditions—Flies were raised on standard cornmeal medium and were maintained at 23 °C, 70% relative humidity, on a 12-h light:12-h dark cycle. The fly strain used in all experiments was *white^{1118}* and was obtained from the Bloomington Stock Center.

Western Blotting—Cell or mitochondrial pellets were lysed in 150 mM NaCl, 20 mM Tris, pH 7.4, 5 mM EDTA-Tris, 10% glycerol, 1% Triton X-100, supplemented with protease and phosphatase inhibitor cocktails (Sigma), and kept on ice for 20 min. Suspensions were then centrifuged at 18,000 $\times$ *g* for 25 min at 4 °C, and the supernatants were solubilized in Laemmli gel sample buffer. For separation of F-ATPase dimers, the Laemmli buffer was directly added to the dimer bands eluted from a BN-PAGE gel. Samples were separated by 15% SDS-PAGE and transferred electrophoretically to nitrocellulose membranes using an SE400 vertical electrophoresis unit (Hoefer). Western blotting was performed in PBS containing 3% nonfat dry milk with polyclonal goat anti-actin (Santa Cruz Biotechnology), polyclonal rabbit anti-caspase-3 (Cell Signaling), monoclonal mouse anti-CyPD (Calbiochem), monoclonal mouse anti-HA (Sigma), monoclonal mouse anti-F-ATPase subunit β (Abcam), polyclonal rabbit anti-MCU (Sigma), or polyclonal rabbit anti-TOM20 (Santa Cruz Biotechnology) antibodies.

BN-PAGE—Pellets of mitochondria isolated from adult *white^{1118}* flies were suspended at 10 mg $\times$ ml^{-1} in 1$\times$ native PAGE sample buffer (Invitrogen) supplemented with protease inhibitor mixture (Sigma), solubilized with 2% (w/v) digitonin, and immediately centrifuged at 100,000 $\times$ *g* for 25 min at 4 °C. The supernatants were supplemented with native PAGE 5% G-250 sample additive (Invitrogen) and quickly loaded onto a blue native polyacrylamide 3–12% gradient gel (Invitrogen). After electrophoresis, gels were processed, and F-ATPase dimers were prepared for bilayer experiments exactly as described (9).

Immunofluorescence—One day before the experiments, stably transfected S_2R^+pActCyPD-HA cells were seeded on sterilized 13-mm round glass coverslips in a 24-well tissue culture plate at 2×10^5 cells/well in 0.5 ml of culture medium. On the day of the experiment, cells were washed once with PBS and incubated for 20 min at room temperature with 0.5 ml of serum-free Schneider's medium supplemented with 1 μg/ml CsH and 100 nM MitoTracker Red CMXRos (Molecular Probes). Cells were fixed with 4% paraformaldehyde for 20 min at room temperature, permeabilized with 50 mM NH_4Cl in PBS + 0.1% Triton X-100 for 5 min at room temperature, and blocked with PBS containing 3% goat serum for 1 h at room temperature with PBS washes between each step. Monoclonal anti-HA (clone HA-7, Sigma) in PBS with 2% goat serum was added, and incubation was carried out overnight at 4 °C. On the next day, cells were washed with PBS, and the immunoreaction was revealed with FITC-conjugated anti-mouse IgG (Fab-specific, Sigma) in PBS with 2% goat serum for 45 min at room temperature. Coverslips were examined with an Olympus epifluorescence microscope at 60$\times$ magnification.

Cell Transfection, Plasmids, and Constructs—A construct of human cyclophilin (CyP) D cDNA carrying a N-terminal mitochondrial targeting sequence from *Drosophila* Hsp60 (a mitochondrial matrix protein) and a C-terminal HA tag was generated by PCR using total cDNA of the human osteosarcoma cell line HQB17 as template. Oligonucleotides were designed using the on-line tool Primer-BLAST (16). Primer sequences were 5′-ctggtaccatgttccgtttgccagtttcgcttgctcgctcctccattagccgccagttggccatgcgcggctatgccaaggatgtgtgcagcaagggctccggcgacccg-3′ (forward) and 5′-ccgagctcttaagcgtaatctggaacatcgtatgggtagctcaactggccacagtctgtgatg-3′ (reverse). To generate a stable polyclonal cell population constitutively expressing human CyPD in *Drosophila* S_2R^+ cells, the construct was inserted into the pAct5c *Drosophila* expression vector under control of the *Dro-*

sophila actin 5c promoter (a gift of M. F. Ceriani, Laboratorio de Genética del Comportamiento, Fundación Instituto Leloir and Instituto de Investigaciones Bioquímicas, Buenos Aires, Argentina) co-transfected with the selection vector pCoPuro (Addgene plasmid 17533), generated by Dr. Francis Castellino (17). Two million cells/well were plated in a 6-well tissue culture plate in 2 ml of culture medium/well. Cells were incubated for 5 h at room temperature and then transfected with the Effectene transfection reagent kit (Qiagen) with a ratio of selection vector (pCoPuro) to expression vector (pActCyPD-HA) of 1:20. After 3 days, the medium was replaced with culture medium containing 8 μg/ml puromycin for selection.

Electrophysiology—Planar lipid bilayer experiments were performed as described in Ref. 18. Briefly, bilayers of 150–200 picofarads capacitance were prepared using purified soybean asolectin. The standard experimental medium was 100 mM KCl, 10 mM Hepes, pH 7.4. All reported voltages refer to the *cis* chamber, zero being assigned to the *trans* (grounded) side. Currents are considered as positive when carried by cations flowing from the *cis* to the *trans* compartment. Freshly prepared F-ATPase dimers were added to the *cis* side. No current was observed when PTP activators were added to the membrane in the absence of F-ATPase dimers. The I-V curve was obtained in the range of −80 to +40 mV from three independent experiments and contained current values that were measured manually ($n > 30$ for each potential) using the PCLAMP8.0 program set. The conductance value thus obtained was 53.0 ± 7.2 pS.

Reagents and Statistics—All chemicals were of the highest purity commercially available. Reported results are typical of at least three replicates for each condition, and error bars refer to the S.E. *p* values were calculated with Student's *t* test.

RESULTS AND DISCUSSION

Drosophila S_2R^+ cells were permeabilized with digitonin and energized with succinate in the presence of ADP and P_i; an ATP-hydrolyzing system was present to maintain constant [ADP] and synchronize F-ATPases in the direction of ATP synthesis. A train of Ca^{2+} pulses was then added to determine the CRC, *i.e.* the threshold matrix Ca^{2+} load necessary to open the mCrC (1) (Fig. 1*A*, *trace a*). Next, we incubated permeabilized S_2R^+ cells in the absence of respiratory substrates, and then energized mitochondria with ATP in the presence of an ATP-regenerating system to maintain constant [ATP] and synchronize F-ATPases in the direction of ATP hydrolysis (Fig. 1*A*, *trace b*). The CRC was much larger in ATP-hydrolyzing than in ATP-synthesizing mitochondria (Fig. 1, compare *traces a* and *b*). Due to formation of glucose-6-P, the concentration of P_i decreases in the ATP synthesis experiments, and conversely, due to hydrolysis of P-creatine, it increases in the ATP-hydrolyzing protocols. However, in the presence of oligomycin, the CRC was only slightly higher than that observed during ATP synthesis (Fig. 1, *trace a′*), and in the presence of 5 mM P_i under conditions of ATP hydrolysis, the CRC was indistinguishable from that observed at 1 mM P_i (Fig. 1, *trace b′*). Thus, the difference between ATP-synthesizing and ATP-hydrolyzing mitochondria cannot be explained by differences in the P_i concentration. Note that the difference in CRC was also not due to different levels of the membrane potential, which was the same in ATP-synthesizing (Fig. 1*B*, *trace a*) and ATP-hydrolyzing mitochondria (Fig. 1*B*, *trace b*), and responded appropriately to oligomycin and uncoupler.

The threshold Ca^{2+} was increased 3-fold in ATP-hydrolyzing relative to ATP-synthesizing mitochondria (Fig. 1*C*), and the effect was not due to the different nucleotide as such because ADP and ATP displayed indistinguishable effects on the CRC when F-ATPase catalysis was blocked with oligomycin in the presence of Mg^{2+}, and mitochondria were energized with succinate (Fig. 1*D*). We could also exclude participation of the endoplasmic reticulum because Ca^{2+} uptake was not observed in the presence of ATP plus oligomycin (results not shown; see Ref. 6). The intriguing effect of enzyme catalysis described in Fig. 1*A* is also observed for the mammalian PTP (6) and represents a first indication that the mCrC may originate from the F-ATPase as well. This effect could be due to the different conformations of F-ATPase during ATP synthesis and hydrolysis (see *e.g.* Ref. 19) and suggests that the sense of rotation of F-ATPase influences the mCrC of *Drosophila* mitochondria, possibly by modulating accessibility of Ca^{2+}-sensitive site(s) that trigger channel opening (20).

The well characterized F-ATPase inhibitor Bz-423 binds the OSCP subunit of the enzyme in mammalian mitochondria (21) and inhibits both ATP synthesis and hydrolysis (22) while sensitizing the PTP to opening (6). Interestingly, the Ca^{2+} load necessary to trigger mCrC opening was decreased by Bz-423 in a concentration-dependent manner (Fig. 1*E*).

CyPD, a key regulator of the mammalian PTP, also binds the OSCP subunit of the F-ATPase, presumably at the same site as Bz-423, because the latter displaces CyPD from the enzyme complex (6). CyPD binding can be selectively inhibited by cyclosporin A (CsA) or by genetic ablation of CyPD, and both manipulations remarkably desensitize the PTP to Ca^{2+} in that its opening requires about twice the Ca^{2+} load necessary to open the PTP in untreated mitochondria (23). The *Drosophila* genome encodes 14 different CyPs (24). *D. melanogaster* CyP1 has an N-terminal sequence that according to Mitoprot (25) confers high probability of mitochondrial import, yet full sequence analysis led to the conclusion that no mitochondrial CyP is present in this species (24). Consistent with this conclusion, we could not detect mitochondrial localization of a CyP1-GFP fusion protein in S_2R^+ cells (results not shown).

We prepared a cDNA construct with an N-terminal *Drosophila* mitochondrial targeting sequence followed by the human CyPD coding sequence and by a C-terminal HA tag. Transfected cells expressed the human CyPD construct, which was recognized by both the CyPD and the HA antibodies, with the increase of molecular weight expected of the HA tag (Fig. 2*A*, *top left panel*). The protein largely localized to mitochondria as judged (i) by Western blot analysis of cytosolic and mitochondrial fractions after subcellular fractionation (Fig. 2*A*, *bottom left panel*); and (ii) by colocalization with MitoTracker Red CMXRos in fixed cells immunostained with a mouse anti-HA antibody followed by a secondary fluoresceinated antibody against mouse IgG (Fig. 2*A*, *right panel*).

Analysis of the CRC in cells co-transfected with the expression vector pActCyPD-HA and the pCoPuro selection vector as compared with cells containing only the selection vector

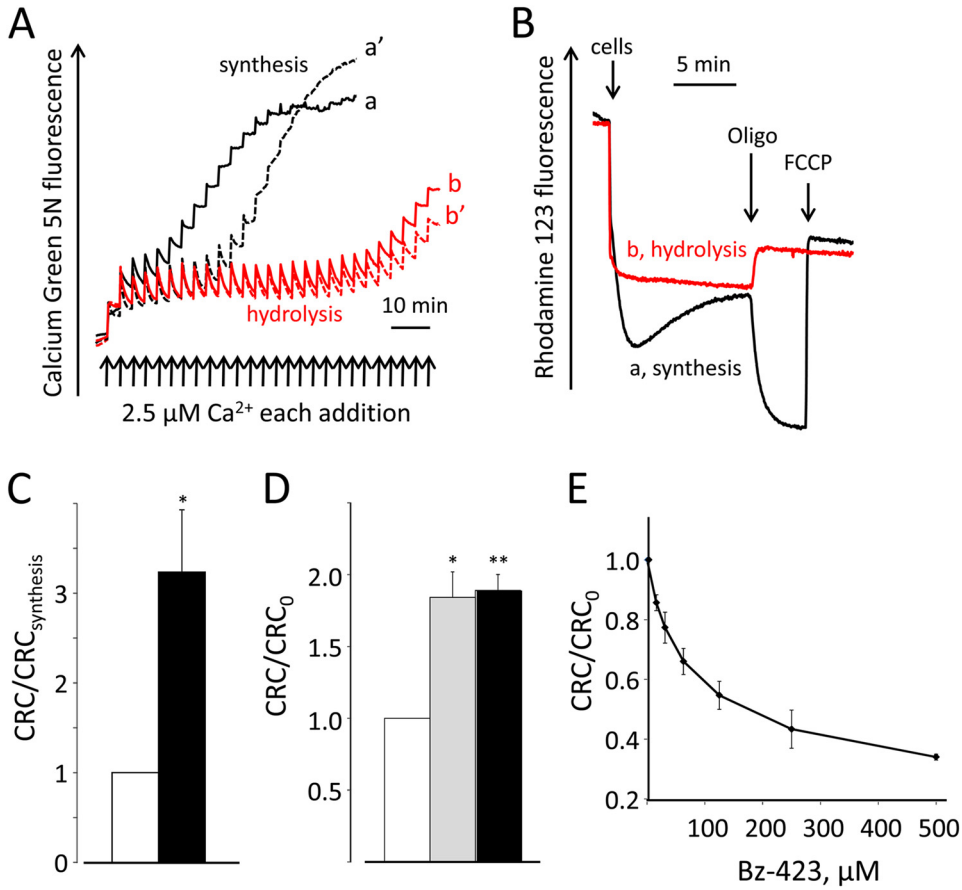

FIGURE 1. **Effect of ATPase catalysis and Bz-423 on the CRC of permeabilized S_2R^+ cells.** *A*, digitonin-permeabilized S_2R^+ cells were incubated as detailed under "Experimental Procedures" either with succinate and ADP plus an ADP-regenerating system in the absence (*trace a*) or presence of 1 μg/ml oligomycin (*trace a'*) or with ATP plus an ATP-regenerating system with 1 mM (*trace b*) or 5 mM P_i (*trace b'*); extramitochondrial Ca^{2+} was monitored with 0.5 μM Calcium Green 5N, and the CRC was determined by the stepwise addition of 2.5 μM Ca^{2+} pulses (*arrows*). *B*, conditions for *traces a* and *b* were as described in the corresponding *traces* of *panel A* except that Calcium Green 5N was replaced with 0.15 μM rhodamine 123; where indicated, 2×10^7 permeabilized S_2R^+ cells, 1 μg/ml oligomycin (*oligo*), and 1 μM carbonylcyanide-*p*-trifluoromethoxyphenyl hydrazone (*FCCP*) were added. *C*, the amount of Ca^{2+} accumulated prior to onset of Ca^{2+}-induced Ca^{2+} release was normalized to that obtained in ATP-synthesizing conditions ($CRC_{synthesis}$) in protocols identical to those of *panel A*; $n = 6$; *, $p < 0.05$. *D*, permeabilized S_2R^+ cells were incubated in 0.1 M sucrose, 80 mM KCl, 10 mM Mops-Tris, pH 7.4, 5 mM succinate-Tris, 4 mM $MgCl_2$, 1 mM P_i-Tris, 10 μM EGTA-Tris, 2 μM rotenone, 1 μg/ml oligomycin, and 0.5 μM Calcium Green 5N, without further additions (*open bar*) or in the presence of 0.4 mM ADP (*gray bar*) or 0.4 mM ATP (*closed bar*). Data are normalized for the CRC determined in the absence of adenine nucleotides (CRC_0); $n = 3$; *, $p < 0.05$, **, $p < 0.005$. *E*, digitonin-permeabilized S_2R^+ cells were incubated in 130 mM KCl, 10 mM Mops-Tris, 5 mM succinate-Tris, 1 mM P_i-Tris, 10 μM EGTA-Tris, 2 μM rotenone, and 0.5 μM Calcium Green 5N in the presence of the stated Bz-423 concentrations. Data are normalized for the CRC obtained in the absence of Bz-423 (CRC_0). *Error bars* in *C–E* indicate S.E.

showed that CyPD expression reduces the threshold Ca^{2+} load required to induce Ca^{2+} release (Fig. 2*B*, compare *traces a* and *b*). The effect of CyPD could not be counteracted by CsA (Fig. 2*B*, *trace c*), however, irrespective of the concentration of P_i (Fig. 2*C*), which in mammalian mitochondria favors CyPD binding to the F-ATPase, resulting in pore sensitization to Ca^{2+} (26, 27). The reason why CsA does not inhibit the mCrC after enforced expression of CyPD remains unclear, but we note (i) that *D. melanogaster* OSCP has a larger number of negative charges in the putative CyPD binding region, which could increase binding affinity; and (ii) that PTP inhibition does not depend on inhibition of CyPD enzymatic activity (28).

At variance from the PTP, the *Drosophila* mCrC is impermeable to sucrose (1). Of note, the size of the *Drosophila* mCrC was unaffected by expression of human CyPD because no Ca^{2+}-induced swelling could be observed after the addition of enough Ca^{2+} to induce mCrC opening (not shown) irrespective of whether naive (Fig. 2*D*, *trace a*) or CyPD-expressing permeabilized cells (Fig. 2*D*, *trace b*) were used. S_2R^+ cells were derived from late embryonic stages (12). To assess whether the low exclusion size and inhibitory response to P_i of the mCrC are restricted to early developmental stages, or rather are defining properties of the *Drosophila* channel, we also measured the swelling response in mitochondria isolated from *white*^{1118} 3rd instar larvae or adult flies. Neither mitochondrial preparation underwent Ca^{2+}-induced swelling, which could instead be readily induced by the addition of the pore-forming peptide alamethicin (Fig. 2*D*, *traces c* and *d*).

In the absence of rotenone, succinate induces reverse electron flow through complex I and leads to generation of reactive oxygen species (29). Rotenone is a potent inhibitor of the mammalian PTP when succinate is used as the substrate (30), and inhibition of reverse electron flow at complex I provides a plausible mechanism for this inhibition because reactive oxygen species increase the probability of pore opening through thiol oxidation (31, 32). Remarkably, rotenone increased nearly 4-fold the CRC of *Drosophila* mitochondria from both larvae and adults (Fig. 2*E*). Thus, lack of swelling after mCrC opening

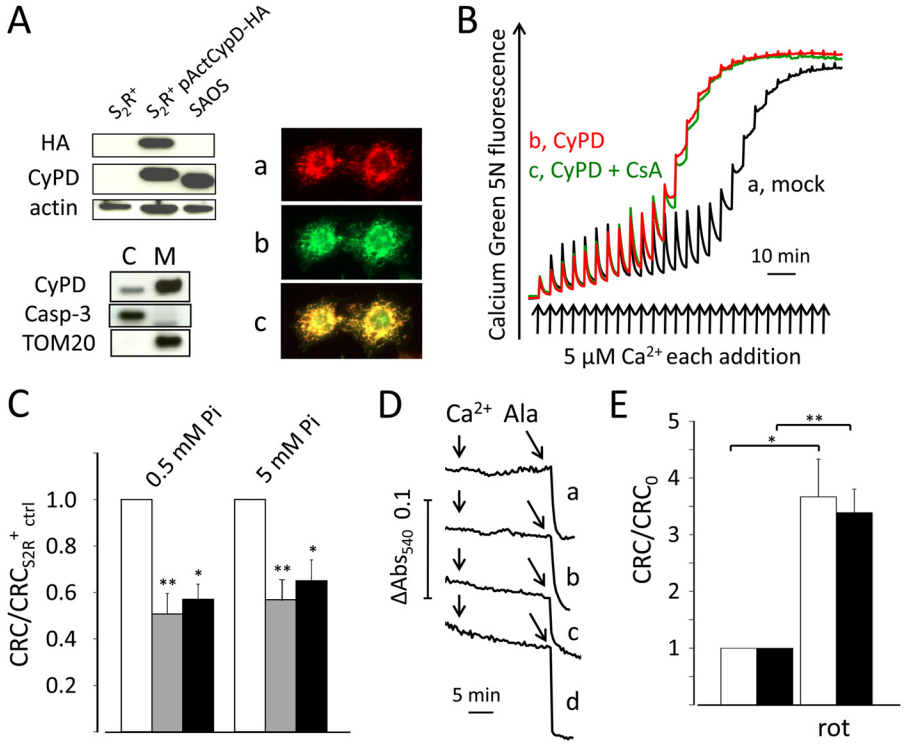

FIGURE 2. **Effect of CyPD expression and rotenone on permeabilized S_2R^+ cells and *Drosophila* mitochondria.** *A*, *top left*, Western blot analysis with antibodies against CyPD, HA, and actin of total cell lysates from non-transfected S_2R^+ cells (S_2R^+), S_2R^+ cells stably transfected with pActCyPD-HA and pCoPuro vectors (S_2R^+ *pActCyPD-HA*), and human SAOS osteosarcoma cells (*SAOS*). *Bottom left*, Western blot analysis with antibodies against CyPD, caspase-3 (*Casp-3*), and TOM20 of cytosolic (*C*) and mitochondrial (*M*) fractions from S_2R^+pActCyPD-HA cells. *Right*, subcellular localization of CyPD in S_2R^+pActCyPD-HA cells determined after staining with MitoTracker Red CMXRos (*panel a*, red fluorescence) and an antibody against the HA tag followed by FITC-conjugated anti-mouse IgG (*panel b*, green fluorescence); the merged image (*panel c*) shows colocalization of the fluorescence signals. *B*, digitonin-permeabilized S_2R^+ cells transfected either with pActCyPD-HA expression vector and pCoPuro selection vector (*trace b*, *CyPD*) or with the selection vector alone (S_2R^+ ctrl, *trace a*, *mock*) were incubated in 250 mM sucrose, 10 mM Mops-Tris, pH 7.4, 5 mM glutamate-Tris, 2.5 mM malate-Tris, 0.5 mM P_i-Tris, 10 μM EGTA-Tris, and 0.5 μM Calcium Green 5N without further additions or in the presence of 0.8 μM CsA (*trace c*, *CyPD + CsA*). Where indicated, 5 μM Ca^{2+} pulses were added (*arrows*). *C*, CRC was measured in S_2R^+ ctrl cells (*open bars*) and in S_2R^+pActCyPD-HA cells in the presence or absence of 0.8 μM CsA (*gray* and *closed bars*, respectively). CRC was normalized to that obtained in non-transfected cells ($CRC_{S2R^+\ ctrl}$); $n = 7$; *, $p < 0.05$, **, $p < 0.005$. *D*, permeabilized S_2R^+ ctrl cells (*trace a*) or S_2R^+pActCyPD-HA cells (*trace b*) were incubated as in *panel B* except that Calcium Green 5N was omitted; mitochondria isolated from *white*^{1118} *Drosophila* 3rd instar larvae (*trace c*), or adult flies (*trace d*) were incubated in 250 mM sucrose, 10 mM Mops-Tris, 5 mM succinate-Tris, 1 mM P_i-Tris, 10 μM EGTA-Tris, 2 μM rotenone, pH 7.4. The Ca^{2+} load necessary to open the mCrC was determined prior to each experiment, and the bolus Ca^{2+} addition was 150% of this amount, *i.e.* 127.5 (*trace a*), 82.5 (*trace b*), 18.8 (*trace c*) or 11.3 μM Ca^{2+} (*trace d*) followed by 10 μM alamethicin (*Ala*). *Abs*, absorbance. *E*, CRC of mitochondria from *white*^{1118} adult flies (*open bars*) or from 3rd instar larvae (*closed bars*) was determined in the absence or presence of 2 μM rotenone (*rot*), and values were normalized to those observed in the absence of rotenone (CRC_0); $n = 5$; *, $p < 0.05$, **, $p < 0.005$. The incubation medium was as in *panel D* except that 0.5 μM Calcium Green 5N was added. *Error bars* in *C* and *E* indicate S.E.

and sensitivity to rotenone are defining features of *Drosophila* mitochondria irrespective of developmental stage.

From these experiments, it appears extremely plausible that the mCrC is the PTP of *Drosophila* mitochondria despite its smaller exclusion size. Given that both the mammalian and yeast F-ATPase form channels (6, 9) whose electrophysiological features are indistinguishable from those of the mitochondrial megachannel (the electrophysiological equivalent of the PTP) (33–38), we next sought to test whether *Drosophila* F-ATPase forms channels, as well as the features of those channels. We purified mitochondria from adult *white*^{1118} flies, separated proteins by BN-PAGE after digitonin extraction, and identified F-ATPase monomers and dimers by in-gel activity staining (Fig. 3*A*, *left lanes*). SDS-PAGE analysis of excised ATPase dimers from the BN-PAGE revealed the typical subunit pattern of the enzyme complex after staining with Coomassie Colloidal Blue (Fig. 3*A*, *middle lanes*). Western blot analysis of the same preparation revealed a lack of contamination by inner membrane MCU and outer membrane TOM20 (Fig. 3*A*, *right lanes*).

The dimer preparation was eluted from the gel and incorporated into asolectin planar bilayers for determination of channel activity (6). The addition of Ca^{2+}, Bz-423, phenylarsine oxide, and copper-*o*-phenanthroline induced opening of a channel with a prevalent single channel conductance of 53 pS (Fig. 3, *B* and *C*), which was consistently observed in different dimer preparations. The addition of γ-imino ATP and Mg^{2+} induced channel closure within a few seconds, as also demonstrated by the amplitude histograms obtained from current traces before and after the addition of the modulators (Fig. 3*C*). Further electrophysiological experiments confirmed that *Drosophila* F-ATPase dimers allow the passage of Ca^{2+} currents (results not shown). Thus, under conditions of oxidative stress and in the presence of Ca^{2+} and Bz-423, the F-ATPase of *Drosophila* forms channels whose conductance is 10-fold smaller than that of the mammalian PTP (6) and 6-fold smaller than that of yeast (9). These features are a perfect match to those defined for the mCrC in permeabilized S_2R^+ cells (1) and leave little doubt that the mCrC is the PTP of *D. melanogaster*. Thus,

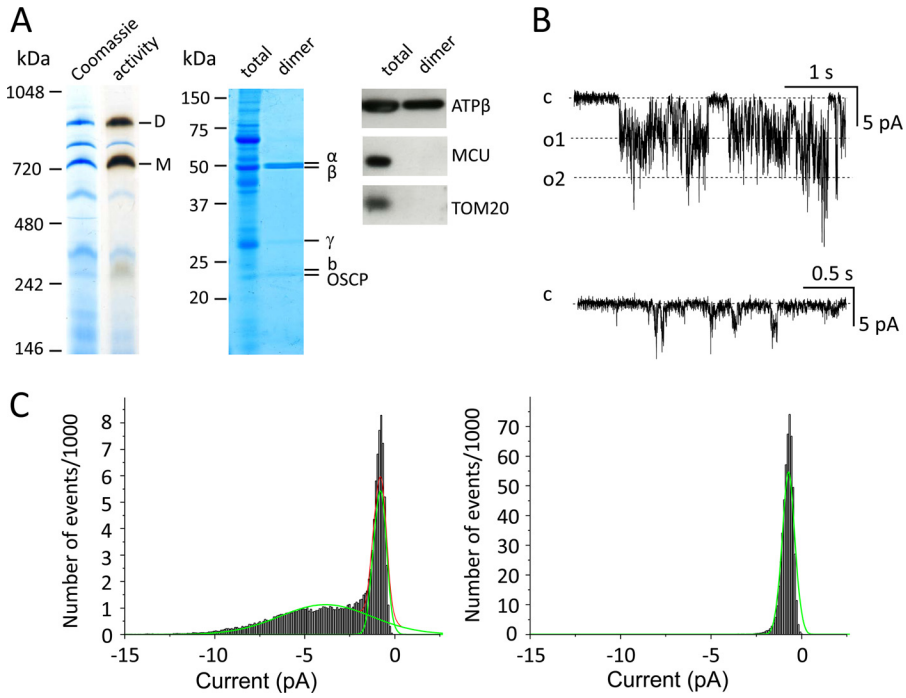

FIGURE 3. **Ca^{2+}-induced currents by F-ATPase dimers reconstituted in planar lipid bilayers.** *A*, mitochondria from adult *white*^{1118} *Drosophila* flies were isolated, extracted with digitonin, and subjected to BN-PAGE as detailed under "Experimental Procedures." *Left lanes*, F-ATPase dimers (*D*) and monomers (*M*) were identified by Coomassie Blue (*Coomassie*) and in-gel activity staining (activity). *Central lanes*, total mitochondrial extracts (*total*) or dimers excised from the BN-PAGE gels (*dimer*) were subjected to SDS-PAGE and stained with colloidal Coomassie Blue; α, β, γ, *b*, and *OSCP* refer to the position of the corresponding subunits of F-ATP synthase. *Right lanes*, Western blot analysis of total lysates (*total*) and F-ATPase dimers (*dimer*) for F-ATPase β subunit (*ATPβ*), MCU, and TOM20. F-ATPase dimers eluted from BN-PAGE (see *left panel*) were incorporated in planar lipid bilayers. *B*, *top recording*, representative current trace recorded at −100 mV (*cis*) (conductance = 53.0 ± 7.2 pS, established from the slope of I-V curves obtained from three independent experiments) following the addition of 2 mM Ca^{2+} plus 0.2 mM phenylarsine oxide, 0.125 mM Bz-423, and 10 μM copper-*o*-phenanthroline (added to the *cis* side) in a medium containing 100 mM KCl, 10 mM Hepes, pH 7.4. *Bottom recording*, effect of 0.8 mM Mg^{2+} (added to the *cis* side) and 0.1 mM γ imino ATP (added to both sides) on channel activity (−100 mV). *C*, amplitude histograms obtained from recordings in the presence of Ca^{2+}, Bz-423, and oxidants (*left panel*) and after the addition of Mg^{2+}/γ imino ATP (*right panel*). Gaussian fittings (*green lines*) were obtained using the Origin 6.1 Program Set.

formation of channels that require Ca^{2+} and oxidation of critical thiol groups is a conserved feature of F-ATPases across species (6, 9, 20).

The finding that the *Drosophila* channel has a unit conductance of 53 pS heavily bears on the nature of the permeability pathway of the PTP. Jonas and co-workers (39) have recently proposed that the pore forms within F_0 after Ca^{2+}-dependent expulsion of F_1, which would then be closed by the β subunit. F_0 is formed by identical c-subunits arranged to form a barrel, the c-ring, whose rotation is tightly linked to the proton gradient. The number of c-subunits per F-ATPase monomer varies between species. In vertebrates and most invertebrates the c-ring has 8 c-subunits, whereas in prokaryotes, chloroplasts and fungi c-rings of 10–15 subunits have been observed (40). The N-terminal α-helix of members with c_8-rings has 3 conserved Ala residues at positions 13, 19, and 23 (bovine numbering), which are essential to avoid side chain clashes (40), and the C-terminal α-helix has 1 conserved Lys residue at position 43, which is trimethylated in humans, pig, sheep and rabbit. This Lys appears to be the binding site for cardiolipin, which allows tight packing of c_8-rings and is essential for enzyme activity and stability (41, 42). All these residues are conserved in *Drosophila* F-ATPase (40), which is consistently affected by cardiolipin loss (43). These structural features indicate that the *Drosophila* complex belongs to the c_8-ring F-ATPase set. It is then difficult to see how a pore forming within c-rings of the same size could mediate formation of a channel with a conductance of 500 pS in mammals and of a mere 53 pS in *Drosophila*, and of 300 pS in yeast where the c-ring has 10 subunits (40). Our findings are therefore not consistent with the idea that PTP channel forms within the c-ring (39), whose actual conductance and Ca^{2+} dependence remain controversial (44–46); see also Refs. 47–49 for discussion.

Given that we readily observe channel formation with F-ATPase dimers but not monomers (6, 9), and that dimerization-resistant yeast strains display resistance to PTP opening (9), our working hypothesis is that the pathway for solute permeation forms between dimers (or higher order structures) (20). Intriguingly, cryoelectron tomography established that F-ATPase dimers from *Drosophila* flight muscle have a unique supramolecular structure, with two parallel rows at the high-curvature edge of cristae vesicles (43). It is possible that this supramolecular assembly prevents formation of high-conductance channels both in the native membrane and during electrophysiological experiments, where dimers could in principle be organized in higher order structures.

Depending on the open time, the mammalian PTP could be involved both in apoptosis induction and in Ca^{2+} homeostasis (50). Prolonged openings cause mitochondrial depolarization, osmotic swelling, outer mitochondrial membrane rupture, and release of apoptogenic proteins such as cytochrome *c*; transient openings, on the other hand, may be involved in physiological

Ca^{2+} homeostasis and may protect mitochondria from Ca^{2+} overload (10, 11), as indicated by studies in isolated cardiomyocytes, CyPD knock-out mice, adult cortical neurons, and spinal chord mitochondria (51–54). It is tempting to speculate that the different PTP conductances observed in mammals, *Drosophila*, and yeast underscore different physiological functions. In particular, due to its smaller size, the *Drosophila* PTP could be involved in Ca^{2+} homeostasis rather than in apoptosis (1, 11), consistent with the finding that the mitochondrial pathway is not essential in most cases of *Drosophila* apoptosis (55–59). The discovery that the *Drosophila* PTP forms from F-ATPase will allow testing of this hypothesis with the powerful methods of *Drosophila* genetics.

REFERENCES

1. von Stockum, S., Basso, E., Petronilli, V., Sabatelli, P., Forte, M. A., and Bernardi, P. (2011) Properties of Ca^{2+} transport in mitochondria of *Drosophila melanogaster*. *J. Biol. Chem.* **286,** 41163–41170
2. Baughman, J. M., Perocchi, F., Girgis, H. S., Plovanich, M., Belcher-Timme, C. A., Sancak, Y., Bao, X. R., Strittmatter, L., Goldberger, O., Bogorad, R. L., Koteliansky, V., and Mootha, V. K. (2011) Integrative genomics identifies MCU as an essential component of the mitochondrial calcium uniporter. *Nature* **476,** 341–345
3. De Stefani, D., Raffaello, A., Teardo, E., Szabò, I., and Rizzuto, R. (2011) A forty-kilodalton protein of the inner membrane is the mitochondrial calcium uniporter. *Nature* **476,** 336–340
4. Palty, R., Silverman, W. F., Hershfinkel, M., Caporale, T., Sensi, S. L., Parnis, J., Nolte, C., Fishman, D., Shoshan-Barmatz, V., Herrmann, S., Khananshvili, D., and Sekler, I. (2010) NCLX is an essential component of mitochondrial Na^+/Ca^{2+} exchange. *Proc. Natl. Acad. Sci. U.S.A.* **107,** 436–441
5. Bernardi, P., and Azzone, G. F. (1983) Regulation of Ca^{2+} efflux in rat liver mitochondria: role of membrane potential. *Eur. J. Biochem.* **134,** 377–383
6. Giorgio, V., von Stockum, S., Antoniel, M., Fabbro, A., Fogolari, F., Forte, M., Glick, G. D., Petronilli, V., Zoratti, M., Szabó, I., Lippe, G., and Bernardi, P. (2013) Dimers of mitochondrial ATP synthase form the permeability transition pore. *Proc. Natl. Acad. Sci. U.S.A.* **110,** 5887–5892
7. Jung, D. W., Bradshaw, P. C., and Pfeiffer, D. R. (1997) Properties of a cyclosporin-insensitive permeability transition pore in yeast mitochondria. *J. Biol. Chem.* **272,** 21104–21112
8. Bradshaw, P. C., and Pfeiffer, D. R. (2013) Characterization of the respiration-induced yeast mitochondrial permeability transition pore. *Yeast* **30,** 471–483
9. Carraro, M., Giorgio, V., Šileikytė, J., Sartori, G., Forte, M., Lippe, G., Zoratti, M., Szabò, I., and Bernardi, P. (2014) Channel formation by yeast F-ATP synthase and the role of dimerization in the mitochondrial permeability transition. *J. Biol. Chem.* **289,** 15980–15985
10. Bernardi, P., and Petronilli, V. (1996) The permeability transition pore as a mitochondrial calcium release channel: a critical appraisal. *J. Bioenerg. Biomembr.* **28,** 131–138
11. Bernardi, P., and von Stockum, S. (2012) The permeability transition pore as a Ca^{2+} release channel: new answers to an old question. *Cell Calcium* **52,** 22–27
12. Schneider, I. (1972) Cell lines derived from late embryonic stages of *Drosophila melanogaster*. *J. Embryol. Exp. Morphol.* **27,** 353–365
13. Yanagawa, S., Lee, J. S., and Ishimoto, A. (1998) Identification and characterization of a novel line of *Drosophila* Schneider S2 cells that respond to Wingless signaling. *J. Biol. Chem.* **273,** 32353–32359
14. Da-Rè, C., von Stockum, S., Biscontin, A., Millino, C., Cisotto, P., Zordan, M. A., Zeviani, M., Bernardi, P., De Pittà, C., and Costa, R. (2014) Leigh syndrome in *Drosophila melanogaster*: morphological and biochemical characterization of Surf1 post-transcriptional silencing. *J. Biol. Chem.* **289,** 29235–29246
15. Fontaine, E., Eriksson, O., Ichas, F., and Bernardi, P. (1998) Regulation of the permeability transition pore in skeletal muscle mitochondria: modulation by electron flow through the respiratory chain complex I. *J. Biol. Chem.* **273,** 12662–12668
16. Ye, J., Coulouris, G., Zaretskaya, I., Cutcutache, I., Rozen, S., and Madden, T. L. (2012) Primer-BLAST: a tool to design target-specific primers for polymerase chain reaction. *BMC Bioinformatics* **13,** 134
17. Iwaki, T., Figuera, M., Ploplis, V. A., and Castellino, F. J. (2003) Rapid selection of *Drosophila* S2 cells with the puromycin resistance gene. *BioTechniques* **35,** 482–484, 486
18. Szabò, I., Soddemann, M., Leanza, L., Zoratti, M., and Gulbins, E. (2011) Single-point mutations of a lysine residue change function of Bax and Bcl-x_L expressed in Bax- and Bak-less mouse embryonic fibroblasts: novel insights into the molecular mechanisms of Bax-induced apoptosis. *Cell Death Differ.* **18,** 427–438
19. Buzhynskyy, N., Sens, P., Prima, V., Sturgis, J. N., and Scheuring, S. (2007) Rows of ATP synthase dimers in native mitochondrial inner membranes. *Biophys. J.* **93,** 2870–2876
20. Bernardi, P. (2013) The mitochondrial permeability transition pore: a mystery solved? *Front. Physiol.* **4,** 95
21. Johnson, K. M., Chen, X., Boitano, A., Swenson, L., Opipari, A. W., Jr., and Glick, G. D. (2005) Identification and validation of the mitochondrial F_1F_0-ATPase as the molecular target of the immunomodulatory benzodiazepine Bz-423. *Chem. Biol.* **12,** 485–496
22. Stelzer, A. C., Frazee, R. W., Van Huis, C., Cleary, J., Opipari, A. W., Jr., Glick, G. D., and Al-Hashimi, H. M. (2010) NMR studies of an immunomodulatory benzodiazepine binding to its molecular target on the mitochondrial F_1F_0-ATPase. *Biopolymers* **93,** 85–92
23. Basso, E., Fante, L., Fowlkes, J., Petronilli, V., Forte, M. A., and Bernardi, P. (2005) Properties of the permeability transition pore in mitochondria devoid of cyclophilin D. *J. Biol. Chem.* **280,** 18558–18561
24. Pemberton, T. J., and Kay, J. E. (2005) Identification and comparative analysis of the peptidyl-prolyl *cis*/*trans* isomerase repertoires of *H. sapiens*, *D. melanogaster*, *C. elegans*, *S. cerevisiae* and *Sz. pombe*. *Comp. Funct. Genomics* **6,** 277–300
25. Claros, M. G., and Vincens, P. (1996) Computational method to predict mitochondrially imported proteins and their targeting sequences. *Eur. J. Biochem.* **241,** 779–786
26. Basso, E., Petronilli, V., Forte, M. A., and Bernardi, P. (2008) Phosphate is essential for inhibition of the mitochondrial permeability transition pore by cyclosporin A and by cyclophilin D ablation. *J. Biol. Chem.* **283,** 26307–26311
27. Giorgio, V., Bisetto, E., Soriano, M. E., Dabbeni-Sala, F., Basso, E., Petronilli, V., Forte, M. A., Bernardi, P., and Lippe, G. (2009) Cyclophilin D modulates mitochondrial F_0F_1-ATP synthase by interacting with the lateral stalk of the complex. *J. Biol. Chem.* **284,** 33982–33988
28. Scorrano, L., Nicolli, A., Basso, E., Petronilli, V., and Bernardi, P. (1997) Two modes of activation of the permeability transition pore: the role of mitochondrial cyclophilin. *Mol. Cell. Biochem.* **174,** 181–184
29. Starkov, A. A. (2008) The role of mitochondria in reactive oxygen species metabolism and signaling. *Ann. N.Y. Acad. Sci.* **1147,** 37–52
30. Li, B., Chauvin, C., De Paulis, D., De Oliveira, F., Gharib, A., Vial, G., Lablanche, S., Leverve, X., Bernardi, P., Ovize, M., and Fontaine, E. (2012) Inhibition of complex I regulates the mitochondrial permeability transition through a phosphate-sensitive inhibitory site masked by cyclophilin D. *Biochim. Biophys. Acta* **1817,** 1628–1634
31. Petronilli, V., Costantini, P., Scorrano, L., Colonna, R., Passamonti, S., and Bernardi, P. (1994) The voltage sensor of the mitochondrial permeability transition pore is tuned by the oxidation-reduction state of vicinal thiols: increase of the gating potential by oxidants and its reversal by reducing agents. *J. Biol. Chem.* **269,** 16638–16642
32. Costantini, P., Chernyak, B. V., Petronilli, V., and Bernardi, P. (1996) Modulation of the mitochondrial permeability transition pore by pyridine nucleotides and dithiol oxidation at two separate sites. *J. Biol. Chem.* **271,** 6746–6751
33. Kinnally, K. W., Campo, M. L., and Tedeschi, H. (1989) Mitochondrial channel activity studied by patch-clamping mitoplasts. *J. Bioenerg. Biomembr.* **21,** 497–506
34. Petronilli, V., Szabò, I., and Zoratti, M. (1989) The inner mitochondrial membrane contains ion-conducting channels similar to those found in bacteria. *FEBS Lett.* **259,** 137–143

35. Szabó, I., and Zoratti, M. (1991) The giant channel of the inner mitochondrial membrane is inhibited by cyclosporin A. *J. Biol. Chem.* **266,** 3376–3379
36. Szabó, I., Bernardi, P., and Zoratti, M. (1992) Modulation of the mitochondrial megachannel by divalent cations and protons. *J. Biol. Chem.* **267,** 2940–2946
37. Bernardi, P., Vassanelli, S., Veronese, P., Colonna, R., Szabó, I., and Zoratti, M. (1992) Modulation of the mitochondrial permeability transition pore: effect of protons and divalent cations. *J. Biol. Chem.* **267,** 2934–2939
38. Szabó, I., and Zoratti, M. (1992) The mitochondrial megachannel is the permeability transition pore. *J. Bioenerg. Biomembr.* **24,** 111–117
39. Alavian, K. N., Beutner, G., Lazrove, E., Sacchetti, S., Park, H. A., Licznerski, P., Li, H., Nabili, P., Hockensmith, K., Graham, M., Porter, G. A., Jr., and Jonas, E. A. (2014) An uncoupling channel within the c-subunit ring of the F_1F_O ATP synthase is the mitochondrial permeability transition pore. *Proc. Natl. Acad. Sci. U.S.A.* **111,** 10580–10585
40. Watt, I. N., Montgomery, M. G., Runswick, M. J., Leslie, A. G., and Walker, J. E. (2010) Bioenergetic cost of making an adenosine triphosphate molecule in animal mitochondria. *Proc. Natl. Acad. Sci. U.S.A.* **107,** 16823–16827
41. Eble, K. S., Coleman, W. B., Hantgan, R. R., and Cunningham, C. C. (1990) Tightly associated cardiolipin in the bovine heart mitochondrial ATP synthase as analyzed by ^{31}P nuclear magnetic resonance spectroscopy. *J. Biol. Chem.* **265,** 19434–19440
42. Gonzalvez, F., D'Aurelio, M., Boutant, M., Moustapha, A., Puech, J. P., Landes, T., Arnauné-Pelloquin, L., Vial, G., Taleux, N., Slomianny, C., Wanders, R. J., Houtkooper, R. H., Bellenguer, P., Møller, I. M., Gottlieb, E., Vaz, F. M., Manfredi, G., and Petit, P. X. (2013) Barth syndrome: cellular compensation of mitochondrial dysfunction and apoptosis inhibition due to changes in cardiolipin remodeling linked to *tafazzin* (TAZ) gene mutation. *Biochim. Biophys. Acta* **1832,** 1194–1206
43. Acehan, D., Malhotra, A., Xu, Y., Ren, M., Stokes, D. L., and Schlame, M. (2011) Cardiolipin affects the supramolecular organization of ATP synthase in mitochondria. *Biophys. J.* **100,** 2184–2192
44. McGeoch, J. E., and Guidotti, G. (1997) A 0.1–700 Hz current through a voltage-clamped pore: candidate protein for initiator of neural oscillations. *Brain Res.* **766,** 188–194
45. McGeoch, J. E., McGeoch, M. W., Mao, R., and Guidotti, G. (2000) Opposing actions of cGMP and calcium on the conductance of the F_0 subunit c pore. *Biochem. Biophys. Res. Commun.* **274,** 835–840
46. McGeoch, J. E., and Guidotti, G. (2001) Batten disease and the control of the F_o subunit c pore by cGMP and calcium. *Eur. J. Paediatr. Neurol.* **5,** Suppl. A, 147–150
47. Bernardi, P., and Di Lisa, F. (2014) The mitochondrial permeability transition pore: molecular nature and role as a target in cardioprotection. *J. Mol. Cell. Cardiol.* **78C,** 100–106
48. Chinopoulos, C., and Szabadkai, G. (2014) What makes you can also break you, Part III: mitochondrial permeability transition pore formation by an uncoupling channel within the C-subunit ring of the F_1F_O ATP synthase? *Front. Oncol.* **4,** 235
49. Rasola, A., and Bernardi, P. (2014) The mitochondrial permeability transition pore and its adaptive responses in tumor cells. *Cell Calcium* **56,** 437–445
50. Petronilli, V., Penzo, D., Scorrano, L., Bernardi, P., and Di Lisa, F. (2001) The mitochondrial permeability transition, release of cytochrome *c*, and cell death: correlation with the duration of pore openings *in situ*. *J. Biol. Chem.* **276,** 12030–12034
51. Altschuld, R. A., Hohl, C. M., Castillo, L. C., Garleb, A. A., Starling, R. C., and Brierley, G. P. (1992) Cyclosporin inhibits mitochondrial calcium efflux in isolated adult rat ventricular cardiomyocytes. *Am. J. Physiol.* **262,** H1699–H1704
52. Elrod, J. W., Wong, R., Mishra, S., Vagnozzi, R. J., Sakthievel, B., Goonasekera, S. A., Karch, J., Gabel, S., Farber, J., Force, T., Brown, J. H., Murphy, E., and Molkentin, J. D. (2010) Cyclophilin D controls mitochondrial pore-dependent Ca^{2+} exchange, metabolic flexibility, and propensity for heart failure in mice. *J. Clin. Invest.* **120,** 3680–3687
53. Barsukova, A., Komarov, A., Hajnóczky, G., Bernardi, P., Bourdette, D., and Forte, M. (2011) Activation of the mitochondrial permeability transition pore modulates Ca^{2+} responses to physiological stimuli in adult neurons. *Eur. J. Neurosci.* **33,** 831–842
54. Parone, P. A., Da Cruz, S., Han, J. S., McAlonis-Downes, M., Vetto, A. P., Lee, S. K., Tseng, E., and Cleveland, D. W. (2013) Enhancing mitochondrial calcium buffering capacity reduces aggregation of misfolded SOD1 and motor neuron cell death without extending survival in mouse models of inherited amyotrophic lateral sclerosis. *J. Neurosci.* **33,** 4657–4671
55. Dorstyn, L., Mills, K., Lazebnik, Y., and Kumar, S. (2004) The two cytochrome *c* species, DC3 and DC4, are not required for caspase activation and apoptosis in *Drosophila* cells. *J. Cell Biol.* **167,** 405–410
56. Means, J. C., Muro, I., and Clem, R. J. (2006) Lack of involvement of mitochondrial factors in caspase activation in a *Drosophila* cell-free system. *Cell Death Differ.* **13,** 1222–1234
57. Oberst, A., Bender, C., and Green, D. R. (2008) Living with death: the evolution of the mitochondrial pathway of apoptosis in animals. *Cell Death Differ.* **15,** 1139–1146
58. Wang, C., and Youle, R. J. (2009) The role of mitochondria in apoptosis. *Annu. Rev. Genet.* **43,** 95–118
59. Xu, D., Woodfield, S. E., Lee, T. V., Fan, Y., Antonio, C., and Bergmann, A. (2009) Genetic control of programmed cell death (apoptosis) in *Drosophila*. *Fly (Austin)* **3,** 78–90